Odontology (2014) 102:98–104
DOI 10.1007/s10266-012-0093-y

ORIGINAL ARTICLE

Characteristics of alveolar bone associated with physiological movement of molar in mice: a histological and histochemical study

Kie Matsuda · Maiko Haga-Tsujimura · Sumio Yoshie · Junko Shimomura-Kuroki

Received: 6 September 2012 / Accepted: 9 November 2012 / Published online: 23 December 2012

Abstract Mouse molars undergo distal movement, during which new bone is formed at the mesial side of the tooth root whereas the preexisting bone is resorbed at the distal side of the root. However, there is little detailed information available regarding which of the bones that surround the tooth root are involved in physiological tooth movement. In the present study, we therefore aimed to investigate the precise morphological differences of the alveolar bone between the bone formation side of the tooth root, using routine histological procedures including silver impregnation, as well as by immunohistochemical analysis of alkaline phosphatase and tartrate-resistant acid phosphatase activity, and immunohistochemical analysis of the expression of the osteocyte markers dentin matrix protein 1, sclerostin, and fibroblast growth factor 23. Histochemical analysis indicated that bone formation by osteoblasts and bone resorption by osteoclasts occurred at the bone formation side and the bone resorption side, respectively. Osteocyte marker immunoreactivity of osteocytes at the surface of the bone close to the periodontal ligament differed at the bone formation and bone resorption sides. We also showed different specific features of osteocytic lacunar canalicular systems at the bone formation and bone resorption sides by using silver staining. This study suggests that the alveolar bone is different in the osteocyte nature between the bone formation side and the bone resorption side due to physiological distal movement of the mouse molar.

Keywords Physiological tooth movement · Osteocyte · Enzyme histochemistry · Immunohistochemistry · Mouse

K. Matsuda
Pediatric Oral Behavior Science, Graduate School of Life Dentistry at Niigata, The Nippon Dental University, Niigata, Japan

M. Haga-Tsujimura · S. Yoshie
Department of Histology, The Nippon Dental University School of Life Dentistry at Niigata, Niigata, Japan

J. Shimomura-Kuroki (✉)
Department of Pediatric Dentistry, The Nippon Dental University School of Life Dentistry at Niigata, 1-8 Hamaura-cho, Chuo-ku, Niigata 951-8580, Japan
e-mail: jshimo@ngt.ndu.ac.jp

Introduction

Mouse molars physiologically move to the distal side of mandible and maxilla [1]. In this distal movement, new bone is formed and the periodontal ligaments thicken at the mesial side of the root (bone formation side); whereas at the alveolar bone of the distal side of the root (bone resorption side), the periodontal ligaments are compressed and the preexisting bone is resorbed [1]. The alveolar bone facing the bone resorption side of the root is resorbed by odontoclasts that are arranged along the tooth surface [1–3]. Moreover, several previous studies have observed that osteoblasts and osteoclasts are present at the bone formation side and the bone resorption side, respectively [4, 5]. These events that occur during physiological tooth movement have been frequently used as a model for study of the mechanisms that underlie orthodontic tooth movement [6, 7].

Mature bone contains an abundance of osteocytes, which extend long cytoplasmic processes that enable cell-to-cell interaction. This cellular network, through which embedded osteocytes and osteoblasts can communicate with each other, is referred to as the osteocytic lacunar canalicular system (OLCS) [8, 9]. Osteocyte function is

associated with bone remodeling and osteocytes are established transducers of the mechanical strain that is translated into biochemical signals that affect the OLCS [8–13]. The distribution of the OLCS within bone was shown to reflect osteocytic function [14], and osteocyte viability is important for the maintenance of bone tissue [13, 15].

Dentin matrix protein 1 (DMP1), sclerostin, and fibroblast growth factor 23 (FGF23) are useful markers of osteocyte function [16–19]. In addition to being specifically expressed by osteocytes, the DMP1 protein is also found in bone matrix and plays a role in bone mineral homeostasis due to its high calcium ion-binding capacity [20]. Sclerostin, which is encoded by the SOST gene, suppresses the activity and viability of osteoblasts and its expression is restricted to osteocytes in mature bone [21, 22]. FGF23 regulates phosphate homeostasis as well as the maintenance of proper mineralization in the bone matrix [23]. The functions of these factors indicate that osteocytes have important roles in bone remodeling. Although there have been some studies of osteoclasts and osteoblasts in the surrounding bone of physiologically distal-moving teeth [1], there are few detailed reports regarding osteocytes in this region.

In this study, we aimed to investigate differences in the morphology of osteocytes at the bone formation side and those at the bone resorption side of the tooth root, that are caused by physiological tooth movement. Osteocytes were detected by immunohistochemical techniques using antibodies against DMP1, sclerostin, and FGF23. In addition, the formation and resorption of alveolar bone around the tooth root was evaluated by histochemical detection of the enzymatic activity of alkaline phosphatase (ALP) and tartrate-resistant acid phosphatase (TRAP), respectively. Histological differences in osteocytes and in osteocytic canaliculi were evaluated by silver impregnation.

Materials and methods

Animals and tissue preparation

This study was approved by the Nippon Dental University ethics commission for animal experimentation. Male ddY-mice (8–11 weeks old, Japan SLC, Inc., Shizuoka, Japan) were used for these experiments. Mice were anesthetized by intraperitoneal injection of sodium pentobarbital (50 mg/kg body weight) and were perfused through the left cardiac ventricle with 4 % paraformaldehyde in 0.1 M phosphate buffer (pH 7.4). Mandibles free of soft tissues were dissected and immersed in the same fixative for an additional 12 h at 4 °C. After decalcification with a solution of 5 % EDTA-2Na (pH 7.4) for 4 weeks at 4 °C, some of the specimens were dehydrated using a graded series of ethanol before embedding in paraffin. Sections (5 μm thick) were made and were stained with hematoxylin and eosin (H-E) or with silver, or were immunohistochemically analyzed. Alternatively, other specimens were immersed overnight at 4 °C in phosphate buffer (pH 7.3) containing 30 % sucrose and were then rapidly frozen in isopentane that was precooled at −35 °C. These specimens were used to make cryosections for histochemical analysis.

Enzyme histochemical analysis

Frozen sections (6 μm thick) were used for the detection of ALP and TRAP activity. ALP activity was detected by incubation of sections with a solution composed of 3 mg of naphthol AS-Mx phosphate disodium salt (Sigma, St. Louis, MO) and 18 mg of fast blue BB salt (Wako, Osaka, Japan) in 15 ml of 0.2 M Tris–HCl buffer (pH 9.0), for 6 min at 37 °C. After rinsing with distilled water, TRAP activity was subsequently detected by incubation of the section with a solution composed of 3 mg of naphthol AS-Mx phosphate (Sigma), 18 mg of fast red violet LB salt (Sigma) and 0.36 g of 50 mM (+) tartaric acid (Wako) in 15 ml of 0.2 M acetate buffer (pH 5.0) for 10 min at 37 °C. After counterstaining with methyl green, the sections were observed and photographed under a conventional light microscope equipped with a digital imaging system (Zeiss, Oberkochen, Germany).

Immunohistochemical analysis

Deparaffinized sections were treated with methanol containing 0.1 % hydrogen peroxide for 30 min, to inhibit endogenous peroxidase, and were then pre-incubated with 1 % bovine serum albumin in phosphate-buffered saline (PBS) for 30 min at room temperature. The sections were subsequently incubated overnight with a rabbit antibody against DMP1 (dilution 1:400, Takara, Otsu, Japan) or with goat anti-sclerostin (dilution 1:30, R&D System Inc., Minneapolis, MN) at 4 °C. After rinsing with PBS, the sections were incubated with horseradish peroxidase (HRP)-conjugated anti-rabbit IgG (Millipore, Billerica, MA) or HRP-conjugated anti-goat IgG (Millipore). Immunoreactions were visualized using a 3,3′-diaminobenzidine substrate kit (Vector Laboratory, Burlingame, CA). For detection of FGF23, deparaffinized sections were treated with a rat anti-FGF23 antibody (dilution 1:100, R&D system Inc.) for 2 h at room temperature. The sections were subsequently incubated with ALP-conjugated goat anti-rat IgG (Seikagaku Biobusiness Co., Tokyo, Japan). To visualize the ALP-conjugated complexes, the treated sections were immersed in an aqueous solution composed of 3 mg of naphthol AS-Mx phosphate (Sigma),

and 18 mg of fast red violet LB salt (Sigma) in 15 ml of 0.2 M Tris–HCl buffer (pH 9.0) for 20 min at 37 °C. All of the sections were counterstained with methyl green, and were observed and photographed as described above.

The specificity of the immunoreactions was checked using the following two negative control experiments: omission of the primary antibodies and the replacement of the primary antibodies with normal sera. These control experiments did not show any specific immunoreaction (data not shown).

In addition, the number of the osteocytes was counted on sclerostin and FGF23 sections under a light microscope (Carl Zeiss) at an original magnification of 200× at the bone formation side and the bone resorption side of the alveolar bone. The observation area was set as a boxed area 0.3 × 0.3 mm in the each side of the alveolar bone. All values were presented as mean ± standard deviation. Data were subjected to Student's *t* test. A *P* value of <0.05 was considered a significant difference.

Silver impregnation

Silver impregnation was performed using a modification of Bodian's protargol-S procedure [14, 18, 24–26]. In brief, the deparaffinized sections were soaked in a 1 % protargol-S solution diluted in borax–boric acid (pH 7.4) for 12–48 h at 37 °C. After rinsing with distilled water, the reaction was enhanced by treatment with an aqueous solution containing 0.2 % hydroquinone, 0.2 % citric acid and 0.7 % nitric silver. After additional rinsing, the sections were treated with a solution of 2.5 % anhydrous sodium sulfate, 0.5 % potassium bromide and 0.5 % amidol diaminophenol dihydrochloride for 5 min. The sections were then treated with 1 % gold chloride, and were subsequently treated with 2 % oxalic acid amidol until black staining of the osteocytic canaliculi was visualized. After rinsing with distilled water, the sections were then fixed in 5 % sodium thiosulfate. These sections were observed and photographed as described above.

Results

Characteristics of the alveolar bone around the tooth root

The histology of the bone formation and bone resorption sides of the interradicular bone of a mouse molar exhibited several characteristic features (Fig. 1a–c).

On the bone formation side, the periodontal ligament was expanded and the surface of the alveolar bone proper, which was invaded by Sharpey's fibers, was smooth in contour (Fig. 1a, b). In addition, a clear reversal line was recognizable between the proper and the supporting alveolar bone (Fig. 1b). In contrast, on the bone resorption side, the periodontal ligament was compressed, the surface of the alveolar bone was irregular in shape, and a few resorption cavities were present (Fig. 1c). The alveolar bone proper was scarcely observed on the bone resorption side and the supporting alveolar bone faced the periodontal ligament in places (Fig. 1c).

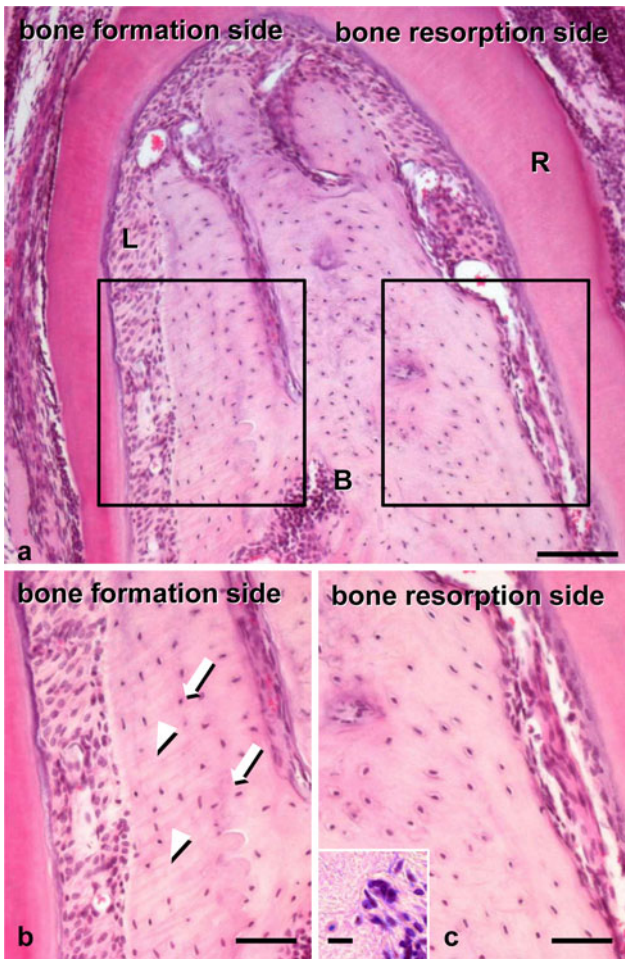

Fig. 1 Comparison of the bone formation and bone resorption sides of an interradicular septum of the first molar alveolar bone using conventional light microscopy. **a** Low magnification overview of a H&E-stained section. *B* alveolar bone, *L* periodontal ligament, *R* tooth root. **b** Magnification of the bone formation side. Sharpey's fibers have invaded the alveolar bone proper (*arrowheads*). A reversal line is recognizable between the alveolar bone proper and the supporting alveolar bone (*arrows*). **c** Magnification of the bone resorption side. A few resorption cavities that include osteoclasts are discernible (*inset*). *Scale bars* 100 μm (**a**), 50 μm (**b**, **c**), 10 μm (**c** *inset*)

To clarify the location of alveolar bone formation and resorption, sections of mandibles containing the molar were double stained for ALP and TRAP activity, which are indicators of bone formation and resorption, respectively (Fig. 2a, b). ALP-positive osteoblasts were present on the surface of the bone and bone marrow at the each side (data

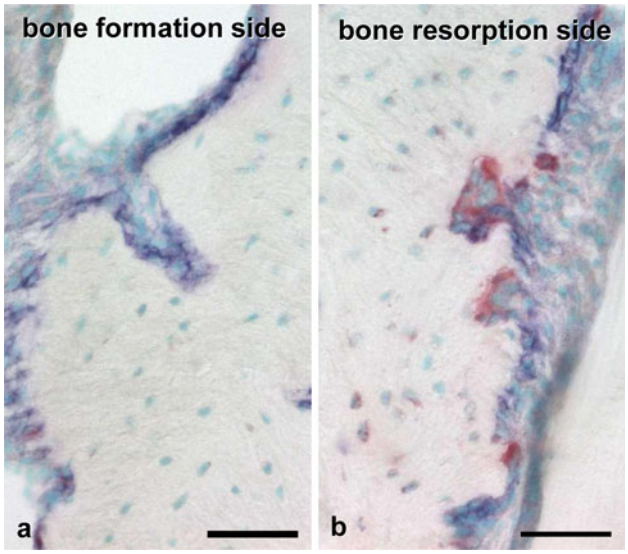

Fig. 2 Double histochemical detection of ALP and TRAP at the bone formation and bone resorption sides. **a** Numerous ALP-positive osteoblasts (*blue*) are observed on the bone surface at the bone formation side. **b** Many TRAP-positive osteoclasts (*red*) are detected on the bone surface on the bone resorption side. Methyl green counterstained. *Scale bars* 50 μm

not shown). In particular, numerous ALP-positive osteoblasts were localized on the surface of the bone on the bone formation side of the interradicular alveolar bone (Fig. 2a). In contrast, many TRAP-positive osteoclasts were observed on the bone resorption side of the interradicular bone of the molar, especially on the bone surface (Fig. 2b).

Analysis of osteocytes and their lacunae and canaliculi

To investigate differences in osteocytic lacunae and canaliculi in the bone formation and bone resorption sides of the alveolar bone, we histologically analyzed bone sections by silver impregnation using a modified Bodian's staining method. Near the surface layer of the bone on the bone formation side, osteocytic canaliculi extended in random directions and osteocytic lacunae were ovoid in shape (Fig. 3a). At the bone resorption side, many flattened osteocytes were observed, while continuity of the canalicular network was lacking in the bone close to the periodontal ligament due to absorption of the bone. In contrast to these features of the bone surface, many osteocytes displayed an ovoid shape inside the bone (Fig. 3b).

Osteocytic lacunae and canaliculi in the entire region of the surrounding bone were immunopositive for DMP1. There was little difference in the expression of DMP1 between the bone formation side and the bone resorption side of the interradicular alveolar bone (Fig. 4a, b).

We further analyzed the expression of sclerostin and FGF23 in osteocytes on the bone formation and bone resorption sides of the tooth root. There were some differences in the distribution of osteocytes that were positively stained with sclerostin and FGF23 between the bone formation side and the bone resorption side of the alveolar bone. Thus, at the bone formation side of the alveolar bone proper, sclerostin was highly expressed in osteocytes in the deep zone, whereas expression of sclerostin was weak in osteocytes in the superficial zone (Fig. 5a). In contrast, on the bone resorption side of the alveolar bone, osteocytes in both the superficial and the deep zones of the bone showed intense sclerostin immunoreactivity (Fig. 5b). In addition, the number of sclerostin-positive osteocytes was significantly higher in the bone resorption side (Fig. 5c).

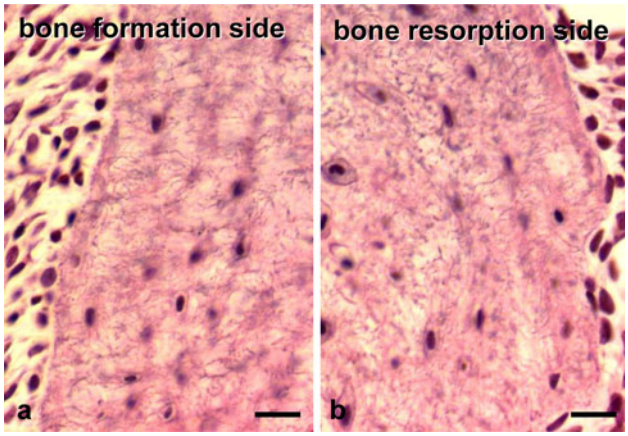

Fig. 3 Silver impregnation of the alveolar bone. **a** The bone formation side. Most of the osteocytes are spindle or ovoid in shape. Osteocytic canaliculi at the surface extend in random directions. **b** The bone resorption side. Many flattened osteocytes are observed near to the bone surface. *Scale bars* 20 μm

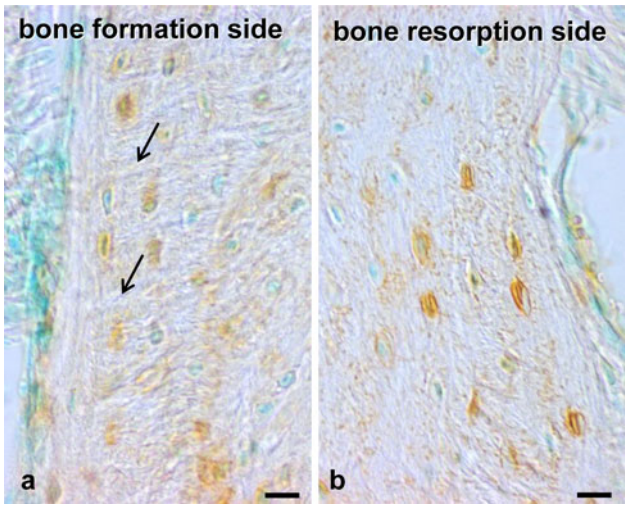

Fig. 4 Immunohistochemistry for DMP1 at the bone formation and resorption sides. **a** The bone formation side. Most of the osteocytes are spindle or ovoid in shape. Sharpey's fibers have invaded the alveolar bone proper (*arrows*). **b** The resorption side. Many flattened osteocytes are observed near the bone surface. *Scale bars* 20 μm

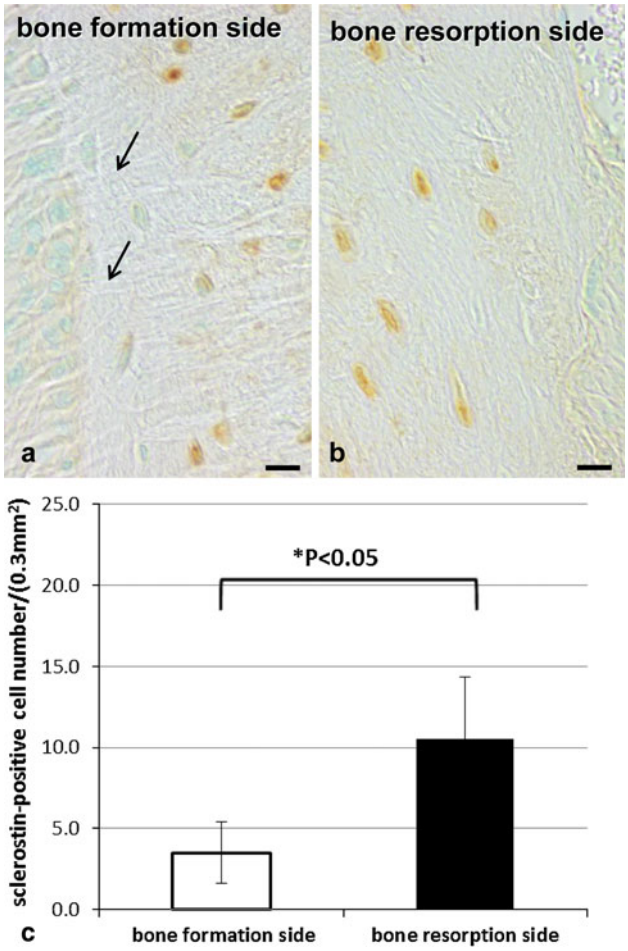

Fig. 5 Immunohistochemical analysis of sclerostin at the bone formation and resorption sides. **a** The bone formation side. Sclerostin-immunopositive osteocytes are localized in the deep zone. Sharpey's fibers have invaded the alveolar bone proper (*arrows*). **b** The bone resorption side. Osteocytes displaying intense sclerostin immunoreactivity are distributed in the superficial and deep zones. Methyl green counterstained. **c** The *graph* shows that the number of sclerostin-positive osteocytes is significantly higher in the bone resorption side. *Scale bars* 20 μm

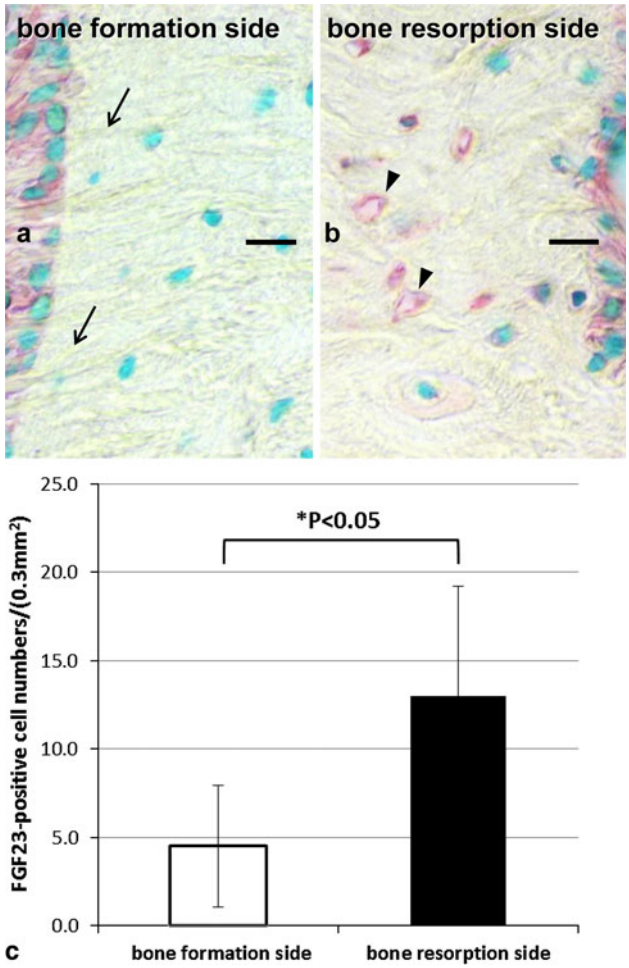

Fig. 6 Immunohistochemical analysis of FGF23 at the bone formation and resorption sides. **a** The bone formation side. Few FGF23-immunoreactive osteocytes are detected in the alveolar bone proper. Osteocytes present in the supporting alveolar bone display intense immunoreactivity. Sharpey's fibers have invaded the alveolar bone proper (*arrows*). **b** The bone resorption side. Osteocytes in the bone surface layer show weak FGF23 immunoreactivity. Osteocytes in the supporting alveolar bone tend to be FGF23-immunopositive (*arrowheads*). Methyl green counterstained. **c** The *graph* shows that the number of FGF23-positive osteocytes is significantly higher in the bone resorption side. *Scale bars* 20 μm

There were few FGF23 immunoreactive osteocytes at the bone formation side of the alveolar bone proper that included Sharpey's fibers. However, osteocytes in the supporting alveolar bone at the bone formation side displayed intense FGF23 immunoreactivity (Fig. 6a). In contrast to osteocytes on the bone formation side, osteocytes on the bone facing the periodontal ligament at the bone resorption side showed faint FGF23 immunoreactivity, while osteocytes within the supporting alveolar bone at the bone resorption side tended to be FGF23 immunopositive (Fig. 6b). The periodontal ligament and the periosteum displayed FGF23 positivity in the bone formation and resorption sides. The number of FGF23-positive osteocytes was significantly higher in the bone resorption side (Fig. 6c).

Discussion

In the present study, using histological analysis, we demonstrated alterations in the surrounding bone of mouse molar during physiological distal tooth movement. This study confirmed formation of bone at the mesial alveolar wall, and resorption of bone at the distal wall of all root surfaces, by double immunohistochemical staining of ALP and TRAP activity. These results are consistent with those reported by Sicher and Weinmann in 1944. In addition, we also observed differences in the OLCS in alveolar bone at the bone formation and bone resorption sides by silver staining. Osteocytes near the bone surface were strongly

influenced by physiological tooth movement and the surrounding bone of the bone formation side had the appearance of woven bone; in contrast, the bone surface at the bone resorption side was irregular in shape. These results indicated that the shape and arrangement of osteocytes in the superficial zone of the bone at the mesial and distal walls of the tooth root were strongly influenced by physiological tooth movement. The results obtained in this study might coincide with to those of a previous study, which postulated that the speed of bone deposition was the most important factor influencing the regularity of the OLCS [18].

Immunohistochemical analysis showed that DMP1-immunopositive osteocytes were distributed throughout the alveolar bone, with no differences observed between the bone formation and bone resorption sides. DMP1 is a bone matrix protein that is expressed in osteocytes and that has been assumed to play a role in bone mineral homeostasis due to its high calcium ion-binding capacity [20]. These data suggest that DMP1 has an important role over a wide area of the surrounding bone of the tooth root during distal movement. Another notable finding of the present study was that osteocytes at both the bone formation and bone resorption sides stained positively for both FGF23 and sclerostin. The only osteocytes that were immunonegative for sclerostin were those in the alveolar proper, near the periodontal ligament. This result may reflect the role of sclerostin, which is known to suppress the activity of osteoblasts and the viability of both osteoblasts and osteocytes [21, 22]. Thus, the restriction of negative immunoreactivity for sclerostin to the specific osteocytes described above supported the idea that osteoblasts are active at the bone formation side, and that physiological tooth movement affects bone remodeling in the surrounding bone that faces onto the periodontal ligament [27]. In addition, few osteocytes in the superficial zone of the bone at the bone formation and bone resorption sides were observed to produce FGF23. In agreement with the fact that FGF23 is produced by osteocytes in organized systems that are associated with proper mineral metabolism [18], osteocytes in the bone surface layer closest to the periodontal ligament were FGF23 immunonegative. These data suggest that the role of osteocytes in the surface of the bone is affected by bone resorption and bone formation, which is then followed by distal movement of the molar. There are no reports concerning FGF23 positivity in the periodontal ligament.

The present study showed that active new bone formation and absorption of the existing bone occurred at the bone formation and the bone resorption sides of alveolar bone, respectively, due to physiological distal movement of a mouse molar. Furthermore, our data regarding osteocyte and bone OLCS morphology suggest that there is a close relationship between the arrangement and the function of osteocytes in bone during physiological movement of a mouse molar.

In conclusion, this study suggests that the alveolar bone is different in the osteocyte nature between the bone formation side and the bone resorption side due to physiological distal movement of the mouse molar.

Acknowledgments The authors thank Professor Norio Amizuka of the Department of Developmental Biology of Hard Tissue, the Graduate School of Dental Medicine, Hokkaido University, and Professor Minqi Li of the School of Stomatology, Shandong University, for their encouragement throughout this study.

Conflict of interest None declared.

References

1. Shicher H, Weinmann JP. Bone growth and physiologic tooth movement. Am J Orthod. 1944;30:109–32.
2. Belting CM, Schour I, Weinmann JP, Shepro MJ. Age changes in the periodontal tissues of the rat molar. J Dent Res. 1953;32:332–53.
3. Macapanpan LC, Weinmann JP. The influence of injury to the periodontal membrane on the spread of gingival inflammation. J Dent Res. 1954;33:263–72.
4. Vignery A, Baron R. Effects of parathyroid hormone on the osteoclastic pool, bone resorption and formation in rat alveolar bone. Calcif Tissue Res. 1978;26:23–8.
5. Yagishita H, Sato K, Warita S, Ando F, Aoba T. Enzyme- and immuno-histochemical studies on root resorption activities accompanied by the physiological and orthodontic tooth movement of rat molars. Jpn J Oral Biol. 2000;42:283–92.
6. Hasegawa K, Yagi T, Ishida T. Electron microscopic observations on root resorption in rat. Jpn J Oral Biol. 1978;20:431–42.
7. Ozawa M. The effect of experimental tooth movement on the root resorption in the maxillary molar teeth of rats. Nihon Kyosei Shika Gakkai Zasshi. 1982;41:616–30.
8. Aarden EM, Burger EH, Nijweide PJ. Function of osteocytes in bone. J Cell Biochem. 1994;55:287–99.
9. Burger EH, Klein-Nulen J. Responses of bone cells to biomechanical forces in vitro. Adv Dent Res. 1999;13:93–8.
10. Lanyon LE. Osteocytes, strain detection, bone modeling and remodeling. Calcif Tissue Int. 1993;53:S102–7.
11. Burger EH, Klein-Nulend J, van der Plas A, Nijweide PJ. Function of osteocytes in bone—their role in mechanotransduction. J Nutr. 1995;125:2020S–3S.
12. Klein-Nulend J, van der Plas A, Semeins CM, Ajubi NE, Frangos JA, Nijweide PJ, Burger EH. Sensitivity of osteocytes to biomechanical stress in vitro. FASEB J. 1995;9:441–5.
13. Knothe Tate ML, Adamson JR, Tami AE, Bauer TW. The osteocyte. Int J Biochem Cell Biol. 2004;36:1–8.
14. Hirose S, Li M, Kojima T, de Freitas PH, Ubaidus S, Oda K, Saito C, Amizuka N. A histological assessment on the distribution of the osteocytic lacunar canalicular system using silver staining. J Bone Miner Metab. 2007;25:374–82.
15. Noble BS, Reeve J. Osteocyte function, osteocyte death and bone fracture resistance. Mol Cell Endocrinol. 2000;159:7–13.
16. Winkler DG, Sutherland MK, Geoghegan JC, Yu C, Hayes T, Skonier JE, Shpektor D, Jonas M, Kovacevich BR, Staehling-Hampton K, Appleby M, Brunkow ME, Latham JA. Osteocyte control of bone formation via sclerostin, a novel BMP antagonist. EMBO J. 2003;22:6267–76.

17. Atkins GJ, Welldon KJ, Holding CA, Haynes DR, Howie DW, Findlay DM. The induction of a catabolic phenotype in human primary osteoblasts and osteocytes by polyethylene particles. Biomaterials. 2009;30:3672–81.
18. Ubaidus S, Li M, Sultana S, de Freitas PH, Oda K, Maeda T, Takagi R, Amizuka N. FGF23 is mainly synthesized by osteocytes in the regularly distributed osteocytic lacunar canalicular system established after physiological bone remodeling. J Electron Microsc. 2009;58:381–92.
19. Kramer I, Keller H, Leupin O, Kneissel M. Does osteocytic SOST suppression mediate PTH bone anabolism? Trends Endocrinol Metab. 2010;21:237–44.
20. Toyosawa S, Shintani S, Fujiwara T, Ooshima T, Sato A, Ijuhin N, Komori T. Dentin matrix protein 1 is predominantly expressed in chicken and rat osteocytes but not in osteoblasts. J Bone Miner Res. 2001;16:2017–26.
21. van Bezooijen RL, Roelen BA, Visser A, van der Wee-Pals L, de Wilt E, Karperien M, Hamersma H, Papapoulos SE, ten Dijke P, Löwik CW. Sclerostin is an osteocyte-expressed negative regulator of bone formation, but not a classical BMP antagonist. J Exp Med. 2004;199:805–14.
22. Lin C, Jiang X, Dai Z, Guo X, Weng T, Wang J, Li Y, Feng G, Gao X, He L. Sclerostin mediates bone response to mechanical unloading through antagonizing Wnt/beta-catenin signaling. J Bone Miner Res. 2009;24:1651–61.
23. Liu S, Quarles LD. How fibroblast growth factor 23 works. J Am Soc Nephrol. 2007;18:1637–47.
24. Bodian D. A new method for staining never fibers and nerve endings in mounted paraffin sections. Anat Rec. 1936;65:89–97.
25. Bodian D. The staining of paraffin sections of nerve tissues with activated protargol. The role of fixatives. Anat Rec. 1937; 69:153–62.
26. Schoen FA. A method to stain decalcified bone without loss of structural detail. Biotech Histochem. 1991;66:216–9.
27. Masuki H, Li M, Hasegawa T, Suzuki R, Ying G, Zhusheng L, Oda K, Yamamoto T, Kawanami M, Amizuka N. Immunolocalization of DMP1 and sclerostin in the epiphyseal trabecule and diaphyseal cortical bone of osteoprotegerin deficient mice. Biomed Res. 2010;31:307–18.